Article

Thiol-Functionalized, 1.5-nm Gold Nanoparticles through Ligand Exchange Reactions: Scope and Mechanism of Ligand Exchange

Gerd H. Woehrle, Leif O. Brown, and James E. Hutchison

J. Am. Chem. Soc., **2005**, 127 (7), 2172-2183• DOI: 10.1021/ja0457718 • Publication Date (Web): 26 January 2005

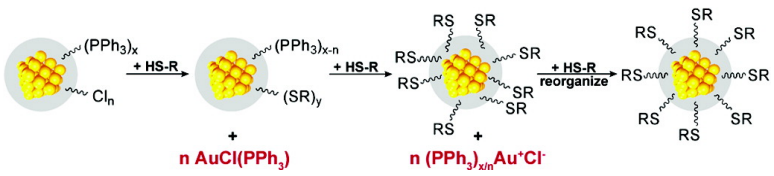

More About This Article

Additional resources and features associated with this article are available within the HTML version:

- Supporting Information
- Links to the 25 articles that cite this article, as of the time of this article download
- Access to high resolution figures
- Links to articles and content related to this article
- Copyright permission to reproduce figures and/or text from this article

View the Full Text HTML

J|A|C|S
ARTICLES
Published on Web 01/26/2005

Thiol-Functionalized, 1.5-nm Gold Nanoparticles through Ligand Exchange Reactions: Scope and Mechanism of Ligand Exchange

Gerd H. Woehrle, Leif O. Brown,† and James E. Hutchison*

Contribution from the Department of Chemistry and Materials Science Institute, 1253 University of Oregon, Eugene, Oregon 97403

Received July 14, 2004; E-mail: hutch@uoregon.edu

Abstract: Ligand exchange reactions of 1.5-nm triphenylphosphine-stabilized nanoparticles with ω-functionalized thiols provides a versatile approach to functionalized, 1.5-nm gold nanoparticles from a single precursor. We describe the broad scope of this method and the first mechanistic investigation of thiol-for-phosphine ligand exchanges. The method is convenient and practical and tolerates a surprisingly wide variety of technologically important functional groups while producing very stable nanoparticles that essentially preserve the small core size and size dispersity of the precursor particle. The mechanistic studies reveal a novel three-stage mechanism that can be used to control the extent of ligand exchange. During the first stage of the exchange, $AuCl(PPh_3)$ is liberated, followed by replacement of the remaining phosphine ligands as PPh_3 (assisted by gold complexes in solution). The final stage involves completion and reorganization of the thiol-based ligand shell.

I. Introduction

Ligand-stabilized nanoparticles have been extensively studied for their use in a large variety of applications, including nanoelectronics,[1,2] nanophotonics,[3] catalysis,[4] sensors,[5] and biotaggents[6] due to their unique physical and chemical properties. For most applications and fundamental studies, it is desirable to be able to tailor the nanoparticle properties by controlling two key structural parameters: (i) the size and composition of the nanoparticle core[7] and (ii) the chemical nature of the stabilizing ligand shell.[8] The size and composition of the nanoparticle core can be used to tune the electronic and optical properties of the nanoparticle. Examples of the importance of the nanoparticle core include the preparation of different-sized semiconductor quantum dots for multicolor optical coding in biological assays[9] and the catalytic oxidation of CO using solid-supported gold nanoparticles of various core sizes.[10] On the other hand, the ligand shell composition allows one to tailor chemical properties such as solubility, chemical reactivity, surface chemistry, and binding affinity. Access to specifically functionalized ligand shells has already resulted in the use of gold nanoparticles in single nucleotide polymorphism detection[11] and as model systems for mimicking glycosphingolipids at cell surfaces.[12]

To provide tailored nanoparticle samples for a wide range of applications, any synthetic method must be convenient and general, in addition to providing nanoparticles with well-defined structures. In some cases, one can control the core size and composition through careful choice of the reaction conditions during synthesis[13,14] or by post-synthetic modifications such as Ostwald ripening[15] and size-selective purification (e.g., fractional crystallization,[16] gel electrophoresis[17]). Despite these advances, precise control over the core size and size dispersity remains a challenge.

Ligand exchange reactions have proven a particularly powerful approach to incorporate functionality in the ligand shell of thiol-stabilized nanoparticles and are widely used to produce

† Present address: Analytical Chemistry Sciences, Los Alamos National Laboratory, Los Alamos, NM 87545.

(1) Berven, C. A.; Clark, L.; Mooster, J. L.; Wybourne, M. N.; Hutchison, J. E. *Adv. Mater.* **2001**, *13*, 109−113.
(2) Sone, J.; Fujita, J.; Ochiai, Y.; Manako, S.; Matsui, S.; Nomura, E.; Baba, T.; Kawaura, H.; Sakamoto, T.; Chen, C. D.; Nakamura, Y.; Tsai, J. S. *Nanotechnology* **1999**, *10*, 135−141.
(3) Maier, S. A.; Brongersma, M. L.; Kik, P. G.; Meltzer, S.; Requicha, A. A. G.; Koel, B. E.; Atwater, H. A. *Adv. Mater.* **2001**, *13*, 1501−1505.
(4) (a) Zhong, C.-J.; Maye, M. M. *Adv. Mater.* **2001**, *13*, 1507−1511. (b) Mohr, C.; Hofmeister, H.; Radnik, J.; Claus, P. *J. Am. Chem. Soc.* **2003**, *125*, 1905−1911.
(5) (a) Zayats, M.; Kharitonov, A. B.; Pogorelova, S. P.; Lioubashevski, O.; Katz, E.; Willner, I. *J. Am. Chem. Soc.* **2003**, *125*, 16006−16014. (b) Willner, I.; Willner, B. *Pure. Appl. Chem.* **2002**, *74*, 1773−1783.
(6) (a) Jahn, W. *J. Struct. Biol.* **1999**, *127*, 106−112. (b) Hainfeld, J. F. *Science* **1987**, *236*, 450−453.
(7) Daniel, M.-C.; Astruc, D. *Chem. Rev.* **2004**, *104*, 293−346.
(8) Warner, M. G.; Hutchison, J. E. In *Functionalization and Surface Treatment of Nanoparticles*; Baraton, M.-I., Ed.; American Scientific Publishers: San Francisco, 2003; pp 67−89.
(9) Han, M.; Gao, X.; Su, J. Z.; Nie, S. *Nat. Biotechnol.* **2001**, *19*, 631−635.
(10) Guczi, L.; Peto, G.; Beck, A.; Frey, K.; Geszti, O.; Molnar, G.; Daroczi, C. *J. Am. Chem. Soc.* **2003**, *125*, 4332−4337.
(11) Sato, K.; Hosokawa, K.; Maeda, M. *J. Am. Chem. Soc.* **2003**, *125*, 8102−8103.
(12) Rojo, J.; Diaz, V.; de la Fuente, J. M.; Segura, I.; Barrientos, A. G.; Riese, H. H.; Bernad, A.; Penades, S. *ChemBioChem* **2004**, *5*, 291−297.
(13) (a) Teranishi, T.; Miyake, M. *Chem. Mater.* **1998**, *10*, 594−600. (b) Hostetler, M. J.; Wingate, J. E.; Zhong, C.-J.; Harris, J. E.; Vachet, R. W.; Clark, M. R.; Londono, J. D.; Green, S. J.; Stokes, J. J.; Wignall, G. D.; Glish, G. L.; Porter, M. D.; Evans, N. D.; Murray, R. W. *Langmuir* **1998**, *14*, 17−30.
(14) Weare, W. W.; Reed, S. M.; Warner, M. G.; Hutchison, J. E. *J. Am. Chem. Soc.* **2000**, *122*, 12890−12891.
(15) (a) Prasad, B. L. V.; Stoeva, S. I.; Sorensen, C. M.; Klabunde, K. J. *Langmuir* **2002**, *18*, 7515−7520. (b) Mohamed, M. B.; Wang, Z. L.; El-Sayed, M. A. *J. Phys. Chem. A* **1999**, *103*, 10255−10259.

10.1021/ja0457718 CCC: $30.25

organic- and water-soluble nanoparticles with various core sizes and functional groups.[8,18] However, this approach continues to be limited by a number of challenges, including difficulties incorporating charged ligands into the ligand shell,[19] controlling the core size independent of the ligand used, and driving complete replacement of the original ligand shell.[18] Direct synthesis approaches have also been employed to prepare functionalized nanoparticles[8,14,20] but most of these methods suffer from the incompatibility of functionalized ligands with the reaction conditions and show a strong dependence of the core size on the stabilizing ligand used during synthesis.[8,21]

We recently developed a novel approach for the preparation of diverse libraries of ligand-stabilized metal nanoparticles that addresses the challenges stated above. It consists of a straightforward two-step procedure, involving (i) preparation of well-defined phosphine-stabilized precursor particles ($d_{CORE} = 1.5 \pm 0.5$ nm)[14,22] and (ii) functionalization of these particles through ligand exchange reactions with ω-functionalized thiols.[23,24] The small set of thiols previously used in this approach suggested that the method might be extended to provide general, convenient access to functionalized, thiol-stabilized gold nanoparticles with a controlled core size. However, the full scope and the mechanism of the ligand exchange approach had not been determined. We anticipate that by understanding the mechanism of the ligand exchange between thiols and phosphine-stabilized gold nanoparticles, the rational development of new synthetic strategies will be facilitated, and the approach will be extended to other materials. Given the potential benefit of such mechanistic studies, it is surprising that only a few studies have been reported to date.[25−28] These studies mainly explore the dynamics of ligand exchange reactions between thiol-stabilized gold nanoparticles and other thiols.[25−27]

Herein, we present a synthetic and mechanistic investigation of the ligand exchange reaction between small, PPh_3-stabilized precursor nanoparticles ($d_{CORE} = 1.5 \pm 0.5$ nm) and ω-functionalized thiols, demonstrating the general nature and full scope of this method. Using this method, we have prepared and fully characterized a wide range of 22 thiol-stabilized gold nanoparticles, incorporating a surprisingly diverse range of functional groups into the ligand shell. The approach provides a convenient route to new materials that have been previously inaccessible and will be a key approach toward the realization of a broad range of applications. In addition, our mechanistic studies of the ligand exchange reaction provide the first fundamental insight into the progression of these types of ligand exchanges. The studies show an unexpected three-stage mechanism that provides valuable insight for further refining the ligand exchange reaction. To this end, we demonstrate that this knowledge allows one to optimize reaction conditions and provides access to novel particles with mixed ligand shells of controlled compositions.

Scheme 1. Ligands Used in the Ligand Exchange Reaction

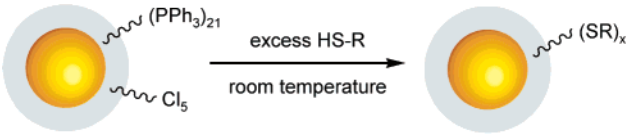

R = $-(CH_2)_nCH_3$ n = 2, 5, 7, 11, 15, 17
-*p*-Ph-OH
-*p*-Ph-CH_3
-*p*-Ph-Ph
$-(CH_2)_3Si(OCH_3)_3$
$-(CH_2)_nCOOH$ n = 1, 2, 6, 11
$-(CH_2CH_2O)_nCH_2CH_2OH$ n = 1, 2
$-(CH_2)_2PO(OH)_2$
$-(CH_2)_2NHMe_2^+ Cl^-$
$-(CH_2)_2NMe_3^+ Cl^-$
$-(CH_2CH_2O)_nCH_2CH_2NMe_3^+ Cl^-$ n = 1,2
$-(CH_2)_2SO_3^- Na^+$

II. Results and Discussion

In the following section, we describe first the scope and broad utility of the ligand exchange method for the preparation of a wide range of small ($d_{CORE} \sim 1.5$ nm), functionalized nanoparticles. We describe functionalization by organic- and water-soluble alkyl- or arylthiols (with neutral or charged headgroups) to illustrate both the ease of preparation and the surprisingly high tolerance of our approach to a large variety of functional groups (Scheme 1). We also discuss convenient purification procedures, the results of complete characterization of these materials, and the important characteristics of the thiol-stabilized nanoparticles obtained by our approach.

In the second part of this section, we describe a mechanistic investigation of the ligand exchange reaction that suggests an unexpected three-stage mechanism for the ligand exchange. Evidence for such a mechanism is derived from product analysis of the ligand exchange reaction, ^{31}P NMR spectroscopy, and trapping experiments to probe for the presence of free PPh_3. The results of these experiments suggest that, initially, the nanoparticles lose triphenylphosphine in the form of AuCl(PPh_3). During the later stages of the exchange, the remaining phosphines are removed as PPh_3 assisted by gold complexes in solution. We also demonstrate how the results from these studies suggest an approach to controlling the extent of the ligand exchange. This makes it possible to synthesize nanoparticles with mixed ligand shells of defined, reproducible composition.

Scope and Utility I: Scope of the Ligand Exchange Reaction. In our previous work, we demonstrated that 1.5-nm triphenylphosphine-stabilized gold nanoparticles (1.5-nm Au_n−

(16) (a) Xia, B.; Lenggoro, I. W.; Okuyama, K. *Chem. Mater.* **2002**, *14*, 2623−2627. (b) Clarke, N. Z.; Waters, C.; Johnson, K. A.; Satherley, J.; Schiffrin, D. J. *Langmuir* **2001**, *17*, 6048−6050.
(17) (a) Schaaff, T. G.; Whetten, R. L. *J. Phys. Chem. B* **2000**, *104*, 2630−2641. (b) Hwang, W.-M.; Lee, C.-Y.; Boo, D. W.; Choi, J.-G. *Bull. Korean Chem. Soc.* **2003**, *24*, 684−686.
(18) Hostetler, M. J.; Green, S. J.; Stokes, J. J.; Murray, R. W. *J. Am. Chem. Soc.* **1996**, *118*, 4212−4213.
(19) (a) Cliffel, D. E.; Zamborini, F. P.; Gross, S. M.; Murray, R. W. *Langmuir* **2000**, *16*, 9699−9702. (b) Templeton, A. C.; Chen, S.; Gross, S. M.; Murray, R. W. *Langmuir* **1999**, *15*, 66−76.
(20) (a) Schmid, G.; Klein, N.; Korste, L.; Kreibig, U.; Schönauer, D. *Polyhedron* **1988**, *7*, 605−608. (b) Schaaff, T. G.; Shafigullin, M. N.; Khoury, J. T.; Vezmar, I.; Whetten, R. L.; Cullen, W. G.; First, P. N.; Gutiérrez-Wing, C.; Ascensio, J.; Yacaman, M. J. *J. Phys. Chem. B* **1997**, *101*, 7885−7891. (c) Templeton, A. C.; Wuelfing, W. P.; Murray, R. W. *Acc. Chem. Res.* **2000**, *33*, 27−36. (d) Brust, M.; Fink, J.; Bethell, D.; Schiffrin, D. J.; Kiely, C. *J. Chem. Soc., Chem. Commun.* **1995**, 1655−1656.
(21) (a) Brust, M.; Walker, M.; Bethell, D.; Schiffrin, D. J.; Whyman, R. *J. Chem. Soc., Chem. Commun.* **1994**, 801−802. (b) Sarathy, K. V.; Raina, G.; Yadav, R. T.; Kulkarni, G. U.; Rao, C. N. R. *J. Phys. Chem. B* **1997**, *101*, 9876−9880.
(22) Hutchison, J. E.; Foster, E. W.; Warner, M. G.; Reed, S. M.; Weare, W. W.; Buhro, W.; Yu, H. *Inorg. Synth.* **2004**, *34*, 228−232.
(23) Brown, L. O.; Hutchison, J. E. *J. Am. Chem. Soc.* **1997**, *119*, 12384−12385.
(24) Warner, M. G.; Reed, S. M.; Hutchison, J. E. *Chem. Mater.* **2000**, *12*, 3316−3320.
(25) Hostetler, M. J.; Templeton, A. C.; Murray, R. W. *Langmuir* **1999**, *15*, 3782−3789.
(26) Montalti, M.; Prodi, L.; Zaccheroni, N.; Baxter, R.; Teobaldi, G.; Zerbetto, F. *Langmuir* **2003**, *19*, 5172−5174.
(27) Ionita, P.; Caragheorgheopol, A.; Gilbert, B. C.; Chechik, V. *J. Am. Chem. Soc.* **2002**, *124*, 9048−9049.
(28) Petroski, J.; Chou, M. H.; Creutz, C. *Inorg. Chem.* **2004**, *43*, 1597−1599.

TPP)[14,29,30] undergo ligand exchange reactions with a few ω-functionalized thiols to produce *functionalized* nanoparticles that preserve the core dimensions of the precursor particles but exhibit highly increased stability against heat, aggregation, and decomposition.[23,24] The development of a convenient synthesis of 1.5-nm Au_n−TPP has generated considerable interest in the ligand exchange reactions of these nanoparticles. To exploit the full potential of this approach, it is necessary to explore its scope and general nature.

In the case of ligand exchanges of thiol-stabilized nanoparticles with free thiols, the use of different ligands can lead to changes in core size, incomplete exchange, or no exchange at all.[18,31] Because one might expect similar outcomes for our method, we investigated a representative family of functionalized thiols for their compatibility with the ligand exchange procedure (Scheme 1).

Ligand exchange between the 1.5-nm Au_n−TPP precursor particle and functionalized thiols can be achieved by combining the phosphine-stabilized nanoparticle with an excess of the thiol (approximately 90−200 molar equivalents with respect to the nanoparticle) in an appropriate solvent. Organic-soluble exchange products are prepared in a monophasic system (typically using CH_2Cl_2 as the solvent) with a variety of alkyl- and arylthiols. We found that the reaction time strongly depends on the thiol ligand used and generally increases with increasing chain length, ranging from 30 min for exchanges with propanethiol up to 18 h for octadecanethiol (ODT). For aromatic thiols, reactions times are usually longer and typically require more than 12 h to achieve complete exchange. This trend in reactivity is consistent with the differences in reactivity for thiol-for-thiol ligand exchange reactions and has mainly been attributed to steric effects.[25]

Water-soluble exchange products can be obtained in a similar fashion using a biphasic solvent system (e.g., CH_2Cl_2−water) in place of the organic solvent. This reaction is applicable for thiols with either neutral or charged (cationic or anionic) headgroups. The trend in reactivity is similar to that of the organic-soluble nanoparticles in that short-chain ligands undergo faster ligand exchange than long-chain ligands. Interestingly, charged ligands generally require considerably shorter reactions times than uncharged ligands in the biphasic reactions. This is possibly due to increased solubility of the partially exchanged particle in the aqueous layer.

As summarized in Scheme 1, the reaction is generally applicable for a wide range of different aliphatic and aromatic thiols and tolerates a surprisingly large number of functional groups, including charged or polar headgroups, such as alcohols, carboxylates, sulfonic acid, phosphonic acid, and ammonium salts. Of the 22 functionalized thiols we tested, all were compatible with this approach, and none resulted in significant core size changes. Most thiols can be exchanged by following a standardized procedure for either monophasic or biphasic reactions. Only a few thiols (e.g., mercaptophenol, mercaptoethanesulfonic acid) required special reaction conditions to achieve complete exchange mainly related to solubility differences between the precursor particle and the exchange product.

Scope and Utility II: Reaction Conditions for Ligand Exchange Reactions. Successful ligand exchange depends on a few general experimental parameters that must be controlled in order to ensure completion of the ligand exchange and avoid decomposition of the 1.5-nm Au_n−TPP precursor particle. The reaction proceeds to completion only when an excess of the incoming thiol is used (approximately 90−200 molar equivalents with respect to the nanoparticle for most thiols). Smaller amounts of thiol usually result in incomplete exchange. On the other hand, if too large an excess of thiol is used (more than 300 molar equivalents in most cases), the phosphine-stabilized nanoparticles rapidly decompose rather than undergoing ligand exchange.[32] Decomposition is also observed when the exchange reaction is carried out at elevated temperatures presumably due to the limited thermal stability of the phosphine-stabilized precursor particles in solution.[30]

In the case of biphasic ligand exchange reactions, it is important to keep the pH of the aqueous phase close to neutral (ideally between pH 5 and 8). Under more acidic conditions (pH 4 and lower) the 1.5-nm Au_n−TPP precursor particles undergo rapid decomposition, significantly reducing the yield of the reaction or preventing ligand exchange completely. At high pH, significant disulfide formation can interfere with ligand exchange unless the reaction is carried out under vigorously oxygen-free conditions. Special attention is also required for ligands with acid headgroups. Unless the ligand exchange is performed at a pH in which such headgroups are completely ionized, an insoluble nanoparticle material forms at the solvent interface consisting of incompletely exchanged nanoparticles. By using slightly basic conditions for the ligand exchange reaction, the formation of insoluble material is avoided and the exchange reaction proceeds to completion. For example, the best results for carboxylic acid terminated alkylthiols (e.g., 3-mercaptopropionic acid) were obtained using a buffered aqueous phase (KH_2PO_4/K_2HPO_4, pH 8). These conditions are basic enough to facilitate the reaction but still close enough to neutral pH to avoid significant disulfide formation (appreciable disulfide formation causes incomplete ligand exchange).

Scope and Utility III: Purification of the Exchange Products. A convenient and rapid purification procedure is necessary if the ligand exchange approach is to be of broad utility. In addition, for a number of applications and studies, it is necessary to obtain high-purity nanoparticle samples. High purity is particularly crucial for studies that investigate structure−function relationships because small amounts of impurities can skew the results. It is therefore important to develop reliable purification methods that are rapid and convenient while at the same time grant high purity. In our initial work,[23] the exchange products were purified through a series of precipitations and/or

(29) The triphenylphosphine-stabilized Au nanoparticles used in this study were prepared according to two different prodecures developed by Schmid et al.[30] and by our group.[22] Both procedures yield nanoparticles with a core size of 1.5 ± 0.5 nm, and both materials have identical optical properties. With the exception of several biphasic ligand exchanges and the trapping studies, all experiments reported herein were carried out using particles prepared by both procedures. We did not observe differences in reactivity between nanoparticles prepared by Schmid's procedure and nanoparticles prepared by our own synthesis. Although different chemical compositions have been reported for both materials (i.e., "$Au_{55}(PPh_5)_{12}Cl_6$" for Schmid's nanoparticles and "$Au_{101}(PPh_3)_{21}Cl_5$" for particles prepared by our synthesis), our experiments show that both materials have the same reactivity. We therefore treat both materials as the same compound and refer to them as 1.5-nm Au_n−TPP for the remainder of the discussion.

(30) Schmid, G.; Pfeil, R.; Boese, R.; Brandermann, F.; Meyer, S.; Calis, G. H. M.; Van der Velden, J. W. A. *Chem. Ber.* **1981**, *114*, 3634−3642.

(31) Templeton, A. C.; Cliffel, D. E.; Murray, R. W. *J. Am. Chem. Soc.* **1999**, *121*, 7081−7089.

(32) Lin, S.-Y.; Tsai, Y.-T.; Chen, C.-C.; Lin, C.-M.; Chen, C.-h. *J. Phys. Chem. B* **2004**, *108*, 2134−2139.

Table 1. Analytical Data for the Ligand Exchange Products

ligand	reaction time	molar equiv of thiol relative to nanoparticles	d_{CORE}[a]	^{1}H NMR chemical shift (ppm); NMR solvent	Au:S ratio[b]	% ligand by mass[c]
$HS(CH_2)_2CH_3$ [d]	30 min	200	1.5 ± 0.4 (N = 952)	1.07 (b); $CDCl_3$ 1.88 (b)	2.3	15.4
$HS(CH_2)_5CH_3$ [d]	4 h	200	1.5 ± 0.3 (N = 1281)	0.90 (b); $CDCl_3$ 1.32 (b) 1.80 (b)	2.3	20.5
$HS(CH_2)_9CH_3$ [d]	8 h	150	1.4 ± 0.4 (N = 786)	0.90 (b); $CDCl_3$ 1.27 (b)	2.3	27.4
$HS(CH_2)_{11}CH_3$ [d]	10 h	125	1.6 ± 0.3 (N = 1180)	0.91 (b); $CDCl_3$ 1.26 (b)	2.3	30.3
$HS(CH_2)_{15}CH_3$ [d]	15 h	100	1.6 ± 0.4 (N = 1024)	0.89 (b); $CDCl_3$ 1.27 (b)	2.3	35.0
$HS(CH_2)_{17}CH_3$ [d]	18 h	90	1.6 ± 0.5 (N = 945)	0.90 (b); $CDCl_3$ 1.26 (b)	2.4	37.1
4-mercaptophenol[d]	12 h[e]	200	1.4 ± 0.4 (N = 1202)	7.23 (b); CD_3OD	2.7	20.1
4-mercaptotoluene[d]	12 h	200	1.5 ± 0.5 (N = 647)	2.21 (b); $CDCl_3$ 7.03 (b)	2.8	21.3
4-mercaptobiphenyl[d]	18 h	140	1.6 ± 0.3 (N = 837)	7.20 (b); $CDCl_3$	2.7	25.5
$HS(CH_2)_3Si(OCH_3)_3$ [d]	6 h	130	1.6 ± 0.4 (N = 771)	3.59 (b); CD_3OD 3.82 (b)	2.5	28.1
$HS(CH_2)COOH$ [f]	2 h	200	1.5 ± 0.3 (N = 1281)	3.30 (b); CD_3OD	2.5	16.4
$HS(CH_2)_2COOH$ [f]	2 h	180	1.5 ± 0.3 (N = 821)	2.90 (b); CD_3OD	2.6	17.5
$HS(CH_2)_5COOH$ [f]	4 h	170	1.5 ± 0.4 (N = 673)	2.70 (b); CD_3OD	2.7	22.6
$HS(CH_2)_{11}COOH$ [f]	7 h	110	1.4 ± 0.3 (N = 592)	1.35 (b); CD_3OD 1.61 (b) 2.28 (b)	2.9	30.6
$HS(CH_2)_2O(CH_2)_2OH$ [f]	6 h	200	1.5 ± 0.5 (N = 923)	3.70 (b); D_2O	2.9	18.7
$HS(CH_2)_2O(CH_2)_2O(CH_2)_2OH$ [f]	8 h	155	1.6 ± 0.4 (N = 867)	3.75 (b); D_2O	3.1	21.9
$HS(CH_2)_2PO(OH)_2$ [f]	5 h	180	1.6 ± 0.4 (N = 1045)	3.31 (b); D_2O	2.9	18.8
$HS(CH_2)_2NMe_2{\cdot}HCl$ [f]	1 h	180	1.4 ± 0.6 (N = 581)	2.90 (b); D_2O 3.52 (b)	2.8	20.8
$HS(CH_2)_2NMe_3^+Cl^-$ [f]	3 h	165	1.6 ± 0.5 (N = 843)	3.34 (b); D_2O 3.74 (b)	2.8	23.6
$HS(CH_2)_2O(CH_2)_2NMe_3^+Cl^-$ [f]	4 h	130	1.6 ± 0.5 (N = 732)	3.21 (b); D_2O 3.62 (b)	2.7	28.4
$HS(CH_2)_2O(CH_2)_2O(CH_2)_2NMe_3^+Cl^-$ [f]	5 h	95	1.6 ± 0.4 (N = 853)	3.20 (b); D_2O 3.61 (b) 3.90 (b)	2.7	31.7
$HS(CH_2)_2SO_3^-Na^+$ [g]	12 h	155	1.5 ± 0.3 (N = 1281)	3.31 (b); D_2O	2.6	25.1

[a] Core diameter in nanometers (mean ± std dev) from analysis of representative TEM images. N refers to the number of particles measured. [b] Ratio obtained from quantification of the areas of the XPS signals. [c] Obtained from TGA analysis. [d] Synthesized according to the general procedure for the preparation of organic-soluble nanoparticles. [e] The reaction is carried out in CH_2Cl_2 for 8 h until a black precipitate is formed. The solvent is replaced with methanol and the mixture stirred for an additional 4 h. [f] Synthesized according to the general procedure for the preparation of water-soluble nanoparticles. [g] This material is obtained in a two-step synthesis as described elsewhere.[24]

solvent washes. This purification method is usually sufficient to remove byproducts and impurities (such as excess free ligand and residual gold salts), but it always leads to a noticeable loss of product. Moreover, it is typically necessary to tailor this method to the solubility characteristics and functional groups of each new nanoparticle, making this approach time-consuming, inconvenient, and inefficient.

A more general approach involves the use of gel filtration chromatography with Sephadex LH-20. With this approach, we achieve almost complete recovery of the nanoparticle material, and we are able to remove excess free ligand, byproducts, and residual gold salts in a rapid and efficient fashion. The versatility of the column material allows purification of all exchange product nanoparticles in a wide range of solvents including chlorinated solvents, alcohols, and water using the same support. Therefore, this technique is applicable for both organic- and water-soluble exchange products. Furthermore, the column material can be routinely reused after sufficient rinsing with an appropriate solvent, reducing cost and preventing waste.

For water-soluble exchange products, it is also possible to exploit ultracentrifugation for purification.[33] At 360000*g*, the particles form an oily pellet at the bottom of the tube (after approximately 12 h of centrifugation), which can be separated from the supernatant to remove molecular impurities. Further purification can be accomplished by mixing the pellet with water and repeating the centrifugation process. At least two cycles of centrifugation are typically required because not all supernatant liquid can be removed.[34]

Scope and Utility IV: Characterization of the Exchange Products. Given the importance of structural and compositional parameters and the need to ensure sufficient purity, the thiol-stabilized exchange products were characterized using a combination of analytical tools including nuclear magnetic resonance (NMR) spectroscopy, UV−vis spectroscopy, transmission electron microscopy (TEM), thermogravimetric analysis (TGA), and X-ray photoelectron spectroscopy (XPS). Analytical data for all thiol-stabilized nanoparticles described in this report are summarized in Table 1.

The purity of the exchange products was confirmed by ^{1}H NMR in which the absence of sharp resonances precludes the

(33) Organic-soluble nanoparticles can only be purified by ultracentrifugation if they are soluble in an appropriate solvent that is compatible with available centrifugation tubes (e.g., alcohols, DMF).

(34) Usually ~90−95% of the supernatant can be separated from the oily pellet before losing a significant amount of product.

presence of excess free ligand and residual gold salts (e.g., AuCl(PPh_3) and higher coordinated Au(I) complexes.[35,36] For exchanges involving nonaromatic thiols, ^{1}H NMR can also be used to confirm that the exchange proceeds to completion (as indicated by the absence of the broad aromatic resonance due to the gold-bound phosphines).[37]

The particle core size was initially assessed by UV−vis spectroscopy.[38] The absence of a plasmon resonance in the optical spectra of the exchange products is consistent with the preservation of the small core size (<2 nm) of the phosphine-stabilized precursor particle. This inference is confirmed by measurement of the core sizes from representative TEM images of the nanoparticles.[39] A typical average core size for the exchanged particles (from $N > 500$ particles/sample) is approximately 1.5 ± 0.4 nm (Table 1).

Finally, the chemical composition was quantified by a combination of XPS and TGA. The absence of phosphorus and chlorine signals in the XPS analysis suggests that the ligand exchange reactions are complete and that all phosphine-containing byproducts have been removed.[40] Quantitative XPS analyses give gold-to-sulfur ratios varying from 2.3:1.0 to 3.1:1.0, depending on the ligand. In all cases, these ratios are in good agreement with ratios obtained by TGA. Under the assumption that the nanoparticle core corresponds to approximately 100 gold atoms,[41] these ratios correspond to an average number of 32−45 thiol ligands/nanoparticle.[42] Qualitatively, nanoparticles stabilized with bulkier aromatic thiols and thiols with functional groups (either internal or peripheral) exhibit lower surface coverage than nonfunctionalized alkylthiols.[38]

Scope and Utility V: Characteristics of the Exchange Products. The thiol-stabilized ligand exchange products obtained by our method possess a number of highly desirable properties that set them apart from their phosphine-stabilized precursors and other thiol-stabilized nanoparticles. Our approach yields nanoparticles that exhibit a high stability that is comparable to other thiol-stabilized nanoparticles.[43] This represents a remarkable stability increase in comparison to the phosphine-stabilized precursors which rapidly decompose in solution to (predominantly) AuCl(PPh_3) and Au(0) within a few hours.[30]

In addition, the approach allows for complete ligand exchange, generating thiol-stabilized nanoparticles with a ligand shell containing only one type of thiol. This is in contrast to thiol-for-thiol ligand exchange reactions which typically result in mixed ligand shells.[25,44] Deliberate access to mixed ligand shell compositions can be achieved by using a feedstock of different thiols during the exchange reaction or using an insufficient amount of thiol to complete the ligand exchange. It is also possible to produce mixed ligand shells by using disulfides instead of thiols.[45]

Finally, the small core dimension and narrow size dispersity of the precursor particles is essentially preserved[46] in the exchange products as synthesized. This is especially important for electronic and optical applications that require convenient access to a diverse family of functionalized nanoparticles with controlled physical properties.[1]

Mechanistic Studies I: General Considerations. In the previous section, we illustrated the scope and general nature of the ligand exchange reaction between 1.5-nm Au_n−TPP precursor particles and thiols. We now focus on a detailed mechanistic investigation of the course of these reactions to learn more about the fundamental reactivity of this important class of nanomaterials. We present an analysis of the products and byproducts of the exchange reaction between Au_n−TPP and ODT using NMR spectroscopy to monitor each species throughout the course of the reaction. These studies are accompanied by trapping experiments designed to probe the fate of the exchanged PPh_3 ligands. A second series of NMR experiments gives detailed insight into the progression of the ligand exchange. We show that the results of this study can be used in combination with the product analysis studies to control the ligand shell composition of the nanoparticles by partially blocking the exchange. Finally, we propose a three-stage mechanistic model for the ligand exchange that is based upon our experimental evidence.[47]

Mechanistic Studies II: Product Analysis of the Ligand Exchange Reaction of 1.5-nm Au_n−TPP with Alkyl Thiols. During our initial studies of the ligand exchange reaction between 1.5-nm Au_n−TPP and thiols, we observed that AuCl(PPh_3)[48] and polyphosphine gold(I) complexes (i.e., $(PPh_3)_n$AuCl) are the main identifiable phosphine-containing products

(35) Attar, S.; Bearden, W. H.; Alcock, N. W.; Alyea, E. C.; Nelson, J. H. *Inorg. Chem.* **1990**, *29*, 425−433.
(36) Terrill, R. H.; Postlethwaite, T. A.; Chen, C.-h.; Poon, C.-D.; Terzis, A.; Chen, A.; Hutchison, J. E.; Clark, M. R.; Wignall, G.; Londono, J. D.; Superfine, R.; Falvo, M.; Johnson, C. S. H., Jr.; Samulski, E. T.; Murray, R. W. *J. Am. Chem. Soc.* **1995**, *117*, 12537−12548.
(37) Sometimes (especially in monophasic exchanges using organic-soluble thiols) a small broad signal centered around 7.5 ppm can be seen which corresponds to unexchanged phosphines or AuCl(PPh_3) impurities. On the basis of integration of the NMR signals, less than ∼3% phosphines (with respect to the thiols) are present in these cases. XPS analysis shows only trace amounts of AuCl(PPh_3) (on the basis of the Au 4f signal) with no detectable phosphorous signal. Free thiol cannot be detected by NMR spectroscopy after successful purification.
(38) See Supporting Information.
(39) Brown, L. O.; Hutchison, J. E. *J. Phys. Chem. B* **2001**, *105*, 8911−8916.
(40) The only exceptions noted to date are the mercaptoethanesulfonate-stabilized nanoparticles, which only partially exchange as reported earlier.[24] However, in this case the ligand exchange can be driven to completion in a subsequent step using a 1:1 water/THF mixture.
(41) On the basis of our previous study,[14] the composition of 1.5-nm Au_n−TPP nanoparticles is approximately $Au_{101}(PPh_3)_{21}Cl_5$. This is in good agreement with theoretical calculations that give 104 core atoms for a 1.5-nm Au particle (using a spherical core geometry).
(42) Using a spherical model for the nanoparticle surface and a footprint for a thiol ligand of ∼0.214 nm^2 (a typical value for alkylthiol SAMS), the surface coverage of the nanoparticles with thiols varies between 78 and 108%. This estimate does not take into account that the different thiols presumably have different footprints and that there are different binding sites on the nanoparticle surface (planes, edges, vertices). For example, a thiol may have a smaller footprint near a facet edge than on a flat surface.
(43) As monitored by UV−vis spectroscopy, the particles do not show any noticeable degradation in solution over extended periods of time (up to several weeks) and can be heated in solution at 75 °C for over 9 h.[23,24] In addition, the water-soluble exchange products reported here show good stability over a wide pH range (typically pH 1−12) and toward high-salt conditions,[24] which makes them suitable for a wide range of applications.
(44) Ingram, R. S.; Hostetler, M. J.; Murray, R. W. *J. Am. Chem. Soc.* **1997**, *119*, 9175−9178.
(45) Wellsted, H.; Sitsen, E.; Caragheorgheopol, A.; Chechik, V. *Anal. Chem.* **2004**, *76*, 2010−2016.
(46) As will be shown in the next section, a small amount of gold atoms (∼5%) is lost during the exchange reaction. However, this loss of core atoms results in an immeasurable change in the particle core diameter.
(47) It is important to note that the present study only investigates ligand exchange reactions with nonpolar ligands in organic solvents. The three-stage mechanism may or may not be applicable to exchanges with polar ligands in aqueous solution.
(48) A complicating factor for the following mechanistic discussion is that samples of 1.5-nm Au_n−TPP always contain trace amounts of AuCl(PPh_3) which can be seen in the UV−visible spectrum.[38] However, the ^{31}P NMR spectrum does not show any peak, suggesting that the amount of AuCl(PPh_3) is either too small to be detected by NMR or that it is involved in an exchange reaction with the nanoparticle. It is possible that the rapid formation of phosphine-rich mixtures of AuCl(PPh_3) described below could be caused in part by the presence of AuCl(PPh_3) in the nanoparticle sample.

Scheme 2. Reactivity of 1-Azido-2,4-Dinitrobenzene with Phosphine-Containing Compounds and the Resulting ^{31}P NMR Chemical Shifts

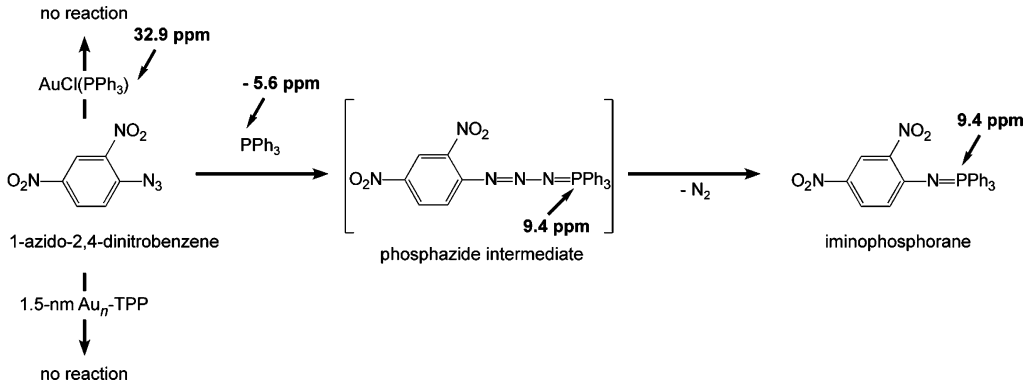

of the ligand exchange. Free PPh_3 was not found in the reaction mixture. This was unexpected because for a simple ligand exchange reaction one might expect that the phosphine ligands dissociate as free PPh_3. This suggested that thiol-for-phosphine exchange reactions follow a significantly different mechanism than thiol-for-thiol exchanges. We therefore designed a series of ^{31}P NMR spectroscopy experiments to study the replacement of the phosphine ligands in detail.

In a first experiment, we investigated the ligand exchange between 1.5-nm Au_n−TPP and ODT using an excess of the thiol (90 molar equivalents ODT with respect to the nanoparticle) to ensure complete exchange. We found that immediately after addition of ODT to the nanoparticle solution (∼1 min), $AuCl(PPh_3)$ was produced as the only observable phosphine-containing species with its characteristic phosphorus chemical shift of 32.9 ppm. The formation of $AuCl(PPh_3)$ as the leaving group of the ligand exchange reaction explains the absence of chlorides in the thiol-stabilized nanoparticles but does not account for all of the phosphine ligands that are replaced by the incoming thiol ligands. The ^{31}P NMR spectrum of the crude reaction mixture after completion of the exchange showed a single, broadened peak at 24.7 ppm. Free PPh_3 was not observed at any stage of the reaction. Even deliberate addition of free PPh_3 to the reaction mixture after completion of the ligand exchange did not lead to the appearance of a resonance for free PPh_3 in the ^{31}P NMR spectrum. Instead, the broadened peak at 24.7 ppm shifted further upfield with increasing addition of free PPh_3.

To understand the results from our product analysis studies, it is important to elucidate the nature of the observed line broadening in the ^{31}P NMR spectra. Line broadening has been observed previously in a number of other studies that investigated the dynamics of ligand exchanges in solutions containing phosphine-stabilized nanoparticles[28,49] and Au(I)−phosphines.[50] On the basis of these studies[28,49,50] and our own experiments, it seems likely that at least two types of reactions can lead to line broadening: (i) exchange between PPh_3 and the phosphine-stabilized nanoparticles and (ii) exchange between PPh_3 and $AuCl(PPh_3)$.

It was recently reported that addition of 1.5-nm Au_n−TPP to a solution of PPh_3 leads to line broadening and a downfield shift of the ^{31}P NMR resonance of PPh_3.[28] The line broadening was explained as a slow ligand exchange between 1.5-nm Au_n−TPP and PPh_3 (the exchange rate was assumed to be in the millisecond regime). The authors also considered that the broadening could be due to the exchange of PPh_3 with $AuCl(PPh_3)$ (always present as an impurity in samples of PPh_3−stabilized nanoparticles) but concluded that this exchange is too rapid and should lead to line narrowing. This conclusion was based upon studies by Schmid et al. who estimated this exchange to be in the microsecond regime.[30,49] However, our own results and a previous report by others[50] suggest that the exchange reaction between PPh_3 and $AuCl(PPh_3)$ leads to line broadening, not to line narrowing. Thus, it appears that ligand exchange between 1.5-nm Au_n−TPP and PPh_3 may be more complex, possibly involving $AuCl(PPh_3)$ in the exchange chemistry. In the present study, thiols bind to the nanoparticle surface, preventing the exchange between PPh_3 or $AuCl(PPh_3)$ with the nanoparticle; thus, the observed line broadening is solely due to the exchange between PPh_3 and $AuCl(PPh_3)$ in the phosphine-rich mixture of $AuCl(PPh_3)$ produced as a result of the ligand exchange. Based upon the ^{31}P NMR chemical shift of the mixture, we can estimate a ratio between PPh_3 and $AuCl(PPh_3)$ of approximately 2.5:1 at the end of the exchange.[38] For a more detailed discussion of phosphine exchange reactions of gold complexes and nanoparticles, see the Supporting Information.

Mechanistic Studies III: Trapping Studies for Free PPh_3 during Ligand Exchange. To understand the fate of the phosphine ligands and to determine if free PPh_3 is produced as a leaving group at any stage, a trapping experiment was performed to assay PPh_3 in solution. The trapping species selected was 1-azido-2,4-dinitrobenzene because it rapidly undergoes a Staudinger reaction with PPh_3,[51] resulting in an iminophosphorane that is easily observable by NMR (see Scheme 2).

We first conducted a series of control experiments to test the ability of the azide (1-azido-2,4-dinitrobenzene) to trap PPh_3 in the presence of $AuCl(PPh_3)$, phosphine-stabilized nanoparticles, alkylthiols, and phosphine-rich mixtures of $AuCl(PPh_3)$. Upon addition of PPh_3 to a solution of $AuCl(PPh_3)$ and the azide, the iminophosphorane (via the phosphazide) was immediately formed and two signals are observed in the $^{31}P\{^1H\}$ NMR spectrum—one corresponding to $AuCl(PPh_3)$ ($\delta = 32.9$ ppm) and one to the iminophosphorane ($\delta = 9.4$ ppm).[52] In contrast, the azide shows no noticeable reaction with solutions of the 1.5-nm Au_n−TPP, $AuCl(PPh_3)$, or ODT over the course of several hours. The azide reacts with phosphine-rich mixtures of $AuCl(PPh_3)$ more slowly and only when an excess of PPh_3

(49) Schmid, G. *Struct. Bonding* **1985**, *62*, 51−85.
(50) Alyea, E. C.; Malito, J.; Attar, S.; Nelson, J. H. *Polyhedron* **1992**, *11*, 2409−2413.
(51) Staudinger, H.; Meyer, J. *Helv. Chim. Acta* **1919**, *2*, 635−646.
(52) No formation of $[Au(PPh_3)_2]^+Cl^-$ is observed in this situation.

(>1 equiv) is present.[38] These controls show that, in a competition experiment, free PPh_3 reacts much faster with the azide than it does with $AuCl(PPh_3)$. However, if PPh_3 is part of a *preexisting* phosphine-rich mixture with $AuCl(PPh_3)$, the azide is unable to compete with $AuCl(PPh_3)$ for PPh_3.

When 1-azido-2,4-dinitrobenzene is added to the ligand exchange mixture of 1.5-nm Au_n−TPP and ODT, free ODT is consumed (as indicated by the disappearance of the methylene resonances closest to the sulfur; see below for details), confirming that the course of the exchange reaction is unaffected by the presence of the azide. Although the ligand exchange proceeds immediately, the azide remains unreacted, until near the end of the reaction when some iminophosphorane is formed. This means that free PPh_3 is not present in solution during the early stages of the reaction. The iminophosphorane produced near the end of the exchange is likely due to the reaction of the azide with the phosphine-rich Au(I) mixture (i.e., mixtures of $AuCl(PPh_3)$ containing PPh_3) that builds up as the reaction proceeds.

A similar product distribution is observed for the decomposition of 1.5-nm Au_n−TPP in the *absence* of thiol.[53] As the nanoparticle decomposes in solution, the UV−visible spectrum displays an increase in absorbance between 230 and 300 nm, consistent with the formation $AuCl(PPh_3)$.[38] However, as in the case of thiol-for-phosphine ligand exchange reactions, $AuCl(PPh_3)$ cannot be the only phosphine-containing product given the phosphine-rich composition of the particle. Trapping studies (to trap free PPh_3) show similar results to thiol-for-phosphine ligand exchange studies and indicate that PPh_3 is not present in solution at any time during decomposition. Instead, the ^{31}P NMR spectrum shows a single, slightly broadened peak that indicates the presence of polyphosphine gold complexes.[50]

If the remaining phosphine ligands are liberated from the nanoparticle as free PPh_3, one would expect immediate formation of iminophosphorane because the trapping reagent is used in excess and reacts much faster with PPh_3 than does $AuCl(PPh_3)$. The lack of iminophosphorane formation until late in the ligand exchange strongly suggests that free PPh_3 is not present in solution. Instead, our results are more consistent with a scenario in which $AuCl(PPh_3)$ (or polyphosphine complexes) associates with the nanoparticle surface and assists directly in the removal of the remaining phosphine ligands, resulting in the formation of polyphosphine Au complexes. In this situation, free PPh_3 is not available in solution and therefore does not react with the azide. The formation of iminophosphorane product toward the end of the reaction results because the excess of PPh_3 over $AuCl(PPh_3)$ becomes high enough so that PPh_3 can be removed from the phosphine-rich $AuCl(PPh_3)$ mixture by the trap. This is in agreement with our observation that the azide forms iminophosphorane with phosphine-rich mixtures of $AuCl(PPh_3)$ very slowly.[38]

Mechanistic Studies IV: Monitoring the Ligand Exchange Reaction by ^{1}H NMR Spectroscopy. The product analysis and trapping studies give important insight into the fate of the phosphines during the ligand exchange process. The experimental evidence suggests that the ligand exchange involves several different stages and is not a simple substitution of the phosphine ligands by thiols. For clarity of the following discussion, we divide ligand exchange into three defined, separate stages. However, one can expect that these stages overlap to a certain extent rather than being strictly separated in time.

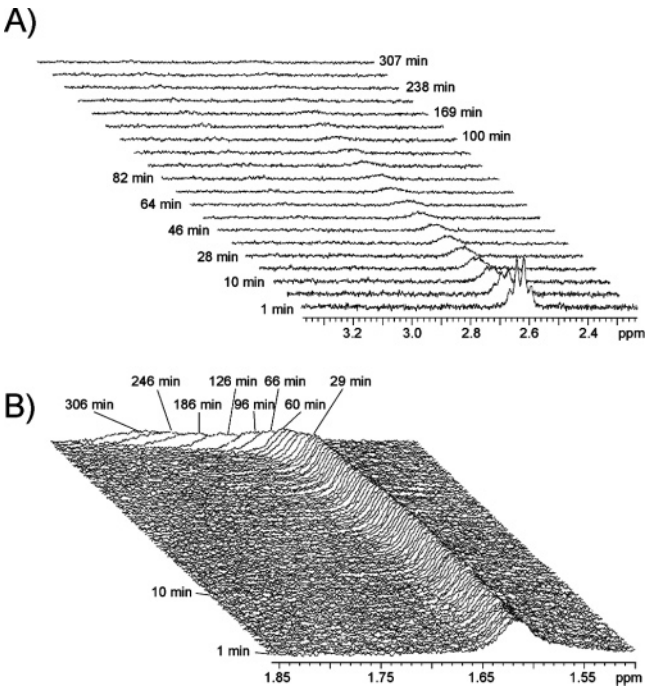

Figure 1. Time evolution of the ligand exchange between 1.5-nm Au_n−TPP (c = 66.7 μmol/L) and ODT (c = 16.7 mmol/L) monitored by ^{1}H NMR spectroscopy (note the nonlinear time scale). (A) α-Methylene resonance of ODT and (B) β-methylene resonance of ODT.

To gain a more detailed understanding about the progression of the ligand exchange, we carried out a series of experiments to monitor the ligand exchange in real time. These studies should not only be interesting from a fundamental point of view but could also provide valuable information that would allow for better control of the ligand exchange.

^{1}H NMR spectroscopy has proven a useful tool to monitor the progression of ligand exchange reactions.[25] Due to significant differences between the ^{1}H NMR spectra of ligand-stabilized nanoparticles and those of the free ligands, NMR spectroscopy can differentiate between unbound free ligand and gold-bound ligand.[38] In comparison to free thiols, the spectrum of thiol-stabilized Au nanoparticles[38] shows significant broadening and a downfield shift for the two methylene resonances closest to the sulfur, as well as a general broadening for the methylene resonances in the chain.[36]

To follow the progression of the exchange reaction by ^{1}H NMR spectroscopy, we performed a ligand exchange experiment for the reaction of 1.5-nm Au_n−TPP with approximately enough ODT to just replace all phosphine ligands. The solution was monitored until no more changes were observed in the ^{1}H NMR spectrum, indicating termination of the exchange. On the basis of the NMR data, we found that the reaction can be divided into three stages that are each accompanied by changes in the ^{1}H NMR spectrum.

During the initial 1−2 min of the reaction (stage 1), the intensity of the α-methylene signal rapidly decreases as ODT is removed from solution and adsorbed onto the nanoparticle surface (Figure 1A). At the same time, a corresponding increase in the concentration of phosphine species in solution is observed,

(53) Decomposition of 1.5-nm Au_n−TPP most likely results in the formation of Au(0) and $AuCl(PPh_3)$.

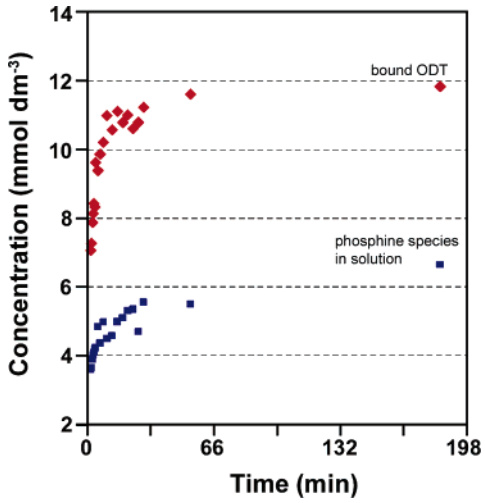

Figure 2. Concentrations of bound ODT (◆) and phosphine-containing species in solution (■) as a function of time during ligand exchange. The concentration of bound ODT was derived from the initial concentration of ODT and the integration ratios of the α-methylene resonance to tetramethylsilane (TMS, internal standard). The concentration of free phosphine in solution was derived from the integration ratio of total free phosphine to TMS.

and the ^{31}P NMR spectrum immediately shows a peak at 32.9 ppm which is characteristic of AuCl(PPh_3). Figure 2 shows the concentration profiles of ODT bound to the nanoparticle and phosphine species in solution. During the first 1−2 min of the exchange, almost half of the total amount of the phosphine species is already liberated. This is consistent with the rapid loss of the total amount of AuCl(PPh_3) and partial removal of the remaining phosphine ligands in the form of Au(I) complexes as described above.

After this initial, fast phase of the reaction, the thiol ligand shell is slowly completed over the course of ∼60 min, which can be followed by a linear downfield shift of the β-methylene protons over time (Figure 1B). During this period, the α-methylene protons are completely broadened into the base line. The concentration profiles show that during this time interval the increase in the phosphine concentration drastically slows down, indicating that essentially all phosphines have been removed from the nanoparticle (Figure 2).

During the final, third stage of the exchange reaction (between ∼60 min and the final measurement), the β-methylene resonance becomes significantly more broadened and continues to shift downfield (Figure 1B).[54] The change is most likely caused by reorganization of ODT into a more crystalline state with specific associated chemical environments for the ligands. This may involve rearrangement of chemisorbed thiolates or loss of hydrogen in a conversion from physisorbed thiol to chemisorbed thiolate.[55] Rearrangement of chemisorbed thiols may help explain the increased reaction time necessary for longer chain thiols. It is quite likely that these processes are also accompanied by a slight rearrangement of the gold core initiated by the loss of Au atoms in the production of AuCl(PPh_3). The observed splitting of the β-methylene signal is believed to correspond to differing binding sites for the thiolates (e.g., faces, edges, and vertices).[56]

Mechanistic Studies V: Partial Inhibition of the Ligand Exchange. All of the experiments described so far suggest that part of the phosphine ligand shell is replaced in the form of AuCl(PPh_3) and not as PPh_3 during the initial stage of the ligand exchange. The remainder of the PPh_3 is lost during later stages of the exchange reaction by a different mechanism involving assisted removal of the ligands by gold complexes in solution. These results pose two fundamental questions: (i) what limits the production of AuCl(PPh_3) and leads to a change in mechanism, and (ii) can this change in mechanism be used to control the extent of ligand exchange by specifically inhibiting part of the exchange reaction?

To answer these two questions, we designed an experiment to block the replacement of the phosphines as PPh_3 by performing an exchange reaction between ODT and 1.5-nm Au_n−TPP in the presence of an excess of PPh_3. Addition of an excess of PPh_3 to the reaction mixture should specifically inhibit the loss of PPh_3 during the later stages of the ligand exchange (as this stage is dependent on the concentration of PPh_3). Loss of AuCl(PPh_3) during the first stage should not be affected because the formation of AuCl(PPh_3) is presumably independent of the concentration of free PPh_3 in solution. The extent of inhibition should allow quantification of the relative amount of AuCl(PPh_3) produced and give insight into what is the limiting factor for the production of AuCl(PPh_3).

The exchange reaction between ODT and 1.5-nm Au_n−TPP was carried out as described in the previous section but with the addition of a 4-fold molar excess of PPh_3 over the amount of ODT. The amount of ODT was chosen to just replace all nanoparticle-bound phosphine ligands. We followed the reaction by ^{1}H NMR spectroscopy and compared it to an identical reaction of ODT with 1.5-nm Au_n−TPP but without adding PPh_3.

The results are summarized in Figure 3 which shows the percentage of ODT in solution over time.[57] Without addition of PPh_3 (Figure 3, ◆) the percentage of unbound ODT rapidly decreases by approximately 60% during the first minute of the reaction (first measurement). The exchange process slows down as the reaction progresses and is complete after approximately 400 min at which time essentially all ODT has been consumed. The situation changes dramatically when excess PPh_3 is added to the exchange reaction (Figure 3, ●). The percentage of free ODT still shows a rapid decrease during the first minutes of the reaction, indicating that the initial stages of the exchange remain largely unaffected by the addition of PPh_3. However, the consumption of free ODT during this initial phase is significantly less than in the absence of PPh_3 (∼15% ODT is immediately consumed). The amount of free ODT in solution slowly stabilizes at approximately 70% after the first 300 min

(54) The ligand exchange is most likely complete at this stage, although some exchange might still take place. The concentration profiles in Figure 2 only show minimal changes in the amount of phosphine species in solution and bound ODT.

(55) The fate of the thiol hydrogen is still a subject of speculation within the literature, but recent experiments show that it is possible to adsorb intact thiols onto Au nanoparticles (with subsequent hydrogen removal) under certain conditions. See: Hasan, M.; Bethell, D.; Brust, M. *J. Am. Chem. Soc.* **2002**, *124*, 1132−1133.

(56) Badia, A.; Gao, W.; Singh, S.; Demers, L.; Cuccia, L.; Reven, L. *Langmuir* **1996**, *12*, 1262−1269.

(57) We used the ratio between the integrals of the α-CH_2 (closest to the sulfur) and the terminal CH_3 as a measure for the amount of ODT in solution. The signal for the α-CH_2 protons disappears when the ligand is bound to the gold surface, whereas the intensity of the signal for the terminal CH_3 remains unchanged.

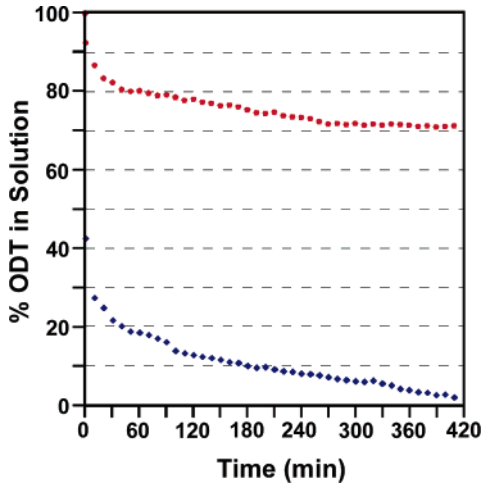

Figure 3. Percentage of ODT in solution to the total amount of ODT added to the ligand exchange reaction as a function of time. The first measurement was taken approximately 60 s after mixing. The diamonds (◆, lower trace) show the profile for the exchange reaction with the stoichiometric amount of ODT added to achieve complete exchange. The circles (●, upper trace) represent the profile of ODT in solution for an identical ligand exchange using a stoichiometric amount of ODT, but in addition an excess of PPh_3 was added to the reaction mixture prior to the exchange. The following concentrations were used: [1.5-nm Au_n−TPP] = 66.7 μmol/L; [ODT] = 16.7 mmol/L; [PPh_3] = 66.7 mmol/L.

of the reaction, indicating that no more thiols are being adsorbed onto the nanoparticle.

The resulting partial inhibition of the ligand exchange by the addition of an excess of PPh_3 is consistent with our observations that $AuCl(PPh_3)$ leaves the nanoparticle as an entity during the first stage of the exchange followed by the loss of PPh_3. On the basis of the extent of ligand exchange still occurring in the presence of excess PPh_3, we can further conclude that the limiting factor for the production of $AuCl(PPh_3)$ is the number of chlorides (i.e., five Cl^-) initially contained in the ligand shell of the phosphine-stabilized precursor nanoparticle. Given the average chemical composition of the nanoparticle ("$Au_{101}(PPh_3)_{21}Cl_5$"), it is expected that approximately 25% of the phosphine ligands can be replaced in the form of $AuCl(PPh_3)$ before all chloride ligands are used up. This is in good agreement with the data presented in Figure 3, showing that approximately 30% of the initial ligand shell is replaced.[58] In addition, XPS data of the partially exchanged nanoparticles shows that approximately 28% of the ligand shell consists of thiols.[59]

The production of nanoparticles with a mixed phosphine/thiol ligand shell (with a controlled ratio) provides a novel route for the synthesis of fully thiol-stabilized nanoparticles that have two different thiols in the ligand shell. Preliminary experiments have shown that the remaining phosphine ligands can be exchanged in a subsequent exchange reaction resulting in the formation of thiol-stabilized nanoparticles with a mixed thiol/thiol ligand shell. We are currently investigating if this route produces thiol-stabilized nanoparticles with a controllable ratio of different thiols.

Mechanistic Studies VI: Proposed Mechanism of the Ligand Exchange Reaction. In the case of thiol-for-thiol ligand exchange reactions, mechanistic studies could be used to determine possible reaction pathways of the exchange reactions and to obtain important information about their dynamics. For example, Murray's studies of the dynamics of thiol-for-thiol ligand exchange reactions on 2−3-nm gold nanoparticles could be used to propose an S_N2-type associative mechanism in which the entering thiol protonates a bound thiolate ligand in the rate-determining step.[25] Evidence that the rate for ligand exchange decreases with increasing length and bulkiness of the incoming thiol ligand further supported this mechanism. These findings were confirmed by Montalti et al. who studied the ligand exchange of pyrene-functionalized nanoparticles with decanethiol using fluorescence spectroscopy.[26] Recently, the ligand exchange reaction with a stable radical-functionalized disulfide was investigated by electron paramagnetic resonance (EPR).[27] The authors proposed a dissociative mechanism based upon their experimental data in which the rate-determining step is the dissociation of a bound thiolate. The proposed mechanism is probably only valid for nanoparticles initially stabilized with weakly bound ligands such as short-chain alkylthiols, amines, and sulfides.

In the present study of thiol-for-phosphine ligand exchange reactions, the NMR product studies and the shapes and chemical shifts of the NMR peaks provide evidence for a three-stage mechanism rather than a pure associative or dissociative mechanism. The proposed mechanism for the ligand exchange reaction of 1.5-nm Au_n−TPP with thiols is shown in Figure 4. As mentioned earlier, the different stages most likely overlap but will be treated separately for clarity. The initial stage of the exchange is characterized by the loss of approximately 25% of the phosphine ligands from the nanoparticle in the form of $AuCl(PPh_3)$. This initial phase is very rapid and is probably completed during the first 1−2 min of the exchange reaction. The loss of $AuCl(PPh_3)$ supports the absence of chloride ligands in the final nanoparticle and indicates a small decrease in the number of core atoms during ligand exchange. Once no more $AuCl(PPh_3)$ can be produced (in which the chloride ligands in the reactant ligand shell are the limiting substituent), the mechanism for the replacement of the phosphine ligands switches and the remaining phosphines are removed in a second stage as PPh_3.

Replacement of phosphines as PPh_3 can occur via one of two possible pathways: In pathway I (Figure 4), the remaining PPh_3 ligands first dissociate from the nanoparticle as free PPh_3 and then rapidly react with $AuCl(PPh_3)$ in solution to form $[Au(PPh_3)_2]^+Cl^-$ or higher gold−phosphine salts. Alternatively (Figure 4, pathway II), PPh_3 is abstracted by direct transfer from the nanoparticle to a closely associated $AuCl(PPh_3)$ in a concerted reaction without ever being free in solution. Both possible pathways result in the same product formation, $[Au(PPh_3)_2]^+Cl^-$ and other multiphosphine gold(I) complexes. On the basis of the trapping experiments (no formation of iminophosphorane until late in the reaction), pathway II appears to be more plausible because PPh_3 is not free in solution at any time during the exchange.

For either pathway I or II, the actual exchange between surface-bound phosphine and thiol could be either associative (with an S_N2-type pathway involving incoming thiol helping to displace the thiol) or dissociative (with an S_N1-type pathway). Supporting evidence for the feasibility of dissociative exchange includes the decomposition of phosphine-stabilized nanoparticles

(58) The error for each data point in Figure 3 was estimated to be roughly ±10% on the basis of difficulties of measuring the integrals exactly due to line broadening and partial signal overlap.
(59) This number was obtained from quantifying the signals for sulfur and phosphorous, which gave a thiol/phosphine ratio of 1.0:2.6.

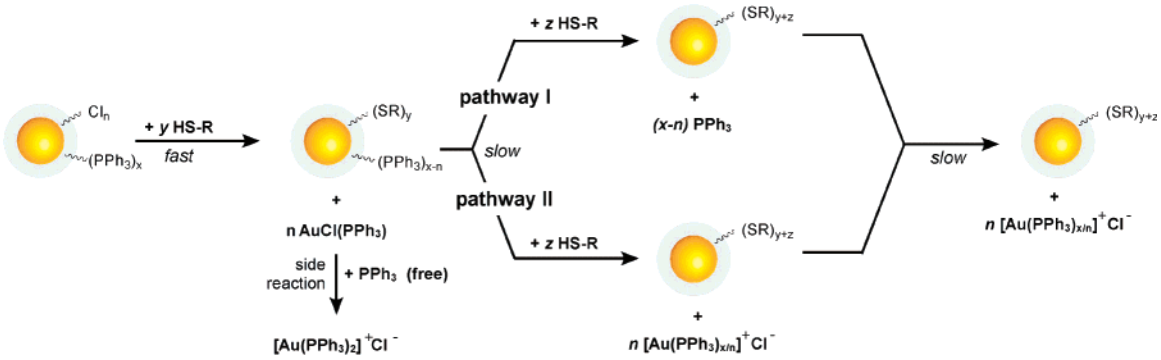

Figure 4. Proposed three-stage mechanism for the ligand exchange reaction between 1.5-nm Au_n−TPP and thiols. In the initial stage, part of the phosphine ligand shell is rapidly replaced in the form of $AuCl(PPh_3)$ until no more particle-bound chlorides are available. This initial phase is followed by removal of the remaining phosphine ligands either as free PPh_3 in solution (pathway I) or through direct transfer of PPh_3 to closely associated $AuCl(PPh_3)$ (pathway II). During the final stage, the completed thiol ligand shell is reorganized into a more crystalline state. Although treated as separate stages, it is most likely that the three stages overlap to a certain extent.

in the absence of thiol.[23,60] Since the product features an increased number of ligands, the complete mechanism must feature addition steps as well as substitution steps.

During the final period of the ligand exchange (Figure 4) the ligand shell is being completed and the thiol ligands are reorganized into a more crystalline state with specific associated chemical environments for the ligands. This stage is characterized by a continued downfield shift and broadening of the β-methylene resonances. As mentioned above, this rearrangement could be a simple rearrangement of chemisorbed thiolates, or it could also involve loss of hydrogen in a conversion from physisorbed thiol to chemisorbed thiolate.

III. Conclusions

The ligand exchange method described in this study offers a general and convenient approach for the preparation of highly functionalized thiol-stabilized gold nanoparticles from a readily accessible phosphine-stabilized precursor nanoparticle. The surprisingly high tolerance for a large variety of technologically important functional groups makes this approach of great interest for many different nanoparticle applications. This approach will prove highly useful by providing convenient access to previously inaccessible nanoparticles in the size regime of 1−2 nm. In combination with the ease of preparation and the defined properties of the resulting thiol-stabilized nanoparticle products (e.g., complete thiol-ligand shell, preservation of the small core size, high stability), we anticipate that the described ligand exchange approach will be of great utility.

The results from our mechanistic studies of the ligand exchange reaction provide detailed insight into the progression of these reactions and revealed an unexpected three-stage mechanism. Apart from this fundamental understanding, the mechanistic studies also have important practical implications for controlling the composition of the ligand shell. The ability to partly block the ligand exchange in a controlled manner opens up new avenues to novel nanoparticles with mixed phosphine/thiol ligand shells. Initial experiments already suggest that such particles can be used themselves as precursors for particles with mixed thiol/thiol ligand shells. This is particularly interesting for numerous applications because it could allow for the preparation of stable nanoparticles that only contained a small but controlled number of functional groups.

IV. Experimental Section

Materials. Hydrogen tetrachloroaurate ($HAuCl_4 \cdot 3H_2O$) was purchased from Strem and was used as received. Dichloromethane was distilled over calcium hydride prior to use. Deuterated chloroform was filtered through a plug of basic alumina prior to use to remove acidic impurities. 1-azido-2,4-dinitrobenzene,[61] 2-(2-mercaptoethoxy)ethanol,[62] and 2-[2-(2-mercaptoethoxy)ethoxy]ethanol[62] were synthesized according to known procedures. All other compounds were purchased from Aldrich Chemical Co. and used as received.

Analytical Procedures. Nuclear magnetic resonance spectra were collected at 25 °C on a Varian Unity Inova 300 MHz instrument equipped with a four-channel probe (^{13}C, 75.42 MHz; ^{31}P, 121.43 MHz). For ^1H and ^{13}C NMR, chemical shifts were referenced to the residual proton resonance of the solvent. For ^{31}P NMR spectroscopy, the spectra were referenced to H_3PO_4 (external standard). X-ray photoelectron spectroscopy was performed on a Kratos Axis HSi instrument operating at a base pressure of $\sim 5 \times 10^{-9}$ mmHg using monochromatic Al Kα radiation at 15 mA and 13.5 kV. Nanoparticle samples were drop-cast from solution onto a clean glass slide. Samples were charge-compensated, and binding energies were referenced to carbon 1s at 284.4 eV. UV−visible spectra were obtained on a Hewlett-Packard 8453 diode array instrument with a fixed slit width of 1 nm using 1-cm quartz cuvettes. Thermal gravimetric analysis was performed on a TA instruments Hi-Res TGA 2950 thermogravimetric analyzer under nitrogen atmosphere (flow rate 100 mL/min). Samples (1−2 mg) were deposited onto Al pans either as powders or by drop-casting from dichloromethane and placed in the instrument until a stable weight was obtained prior to analysis. The samples were heated at a rate of 5 °C/min up to 100 °C, held at that temperature for 15 min to ensure evaporation of all solvent, and then heated to 500 °C at a rate of 5 °C/min. Transmission electron microscopy (TEM) was performed on a Philips CM-12 operating at 120 kV accelerating voltage. Samples were prepared by aerosol deposition of aliquots onto silicon monoxide-coated 400-mesh Cu TEM grids (Ted Pella). Excess solvent was wicked off the grids with filter paper, and the samples were allowed to dry under ambient conditions prior to inspection by TEM. Images were recorded and processed as described previously.[39,63]

(60) Benfield, R. E.; Creighton, J. A.; Eadon, D. G.; Schmid, G. *Z. Phys. D: At., Mol. Clusters* **1989**, *12*, 533−536.
(61) Bailey, A. S.; Case, J. R. *Tetrahedron* **1958**, *3*, 113−131.
(62) Woehrle, G. H.; Warner, M. G.; Hutchison, J. E. *Langmuir* **2004**, *20*, 5982−5988.
(63) Woehrle, G. H.; Hutchison, J. E.; Özkar, S.; Finke, R. G. Submitted for publication.

Synthetic Procedures. (A) Synthesis of Triphenylphosphine-Stabilized Nanoparticles (1.5-nm Au_n−TPP). Triphenylphosphine-stabilized nanoparticles (1.5-nm Au_n−TPP) were synthesized using two different procedures. The first procedure was described by Schmid et al. and employs the reduction of $AuCl(PPh_3)$ with diborane gas.[64] Alternatively, triphenylphosphine-stabilized nanoparticles were synthesized according to a more benign procedure using $NaBH_4$ recently published by our group.[14,22] Both materials had identical spectroscopic properties and reactivities in all experiments.

(B) General Procedure for the Preparation of Organic-Soluble Gold Nanoparticles. To a solution of 20 mg of 1.5-nm Au_n−TPP in dichloromethane (5 mL) was added 20 mg of the organic-soluble thiol ligand.[65] The mixture was stirred rapidly at room temperature until completion of the ligand exchange reaction. The reaction time depends on the incoming ligand and varies from 30 min for propanethiol up to 18 h for long-chain alkylthiols. Upon completion of the exchange reaction the solvent was removed under a stream of nitrogen at room temperature. The crude material was dissolved in the minimum amount of dichloromethane and purified by column chromatography using Sephadex LH-20 to remove byproducts and excess free ligand. The purity of the product (as indicated by the absence of free ligand or molecular gold species) is determined by ^{1}H NMR spectroscopy, and the material can be further characterized by UV−vis spectroscopy, XPS, TGA, and TEM.

(C) General Procedure for the Preparation of Water-Soluble Gold Nanoparticles. To a solution of 20 mg of 1.5-nm Au_n−TPP in dichloromethane (3 mL) was added an aqueous solution of 20 mg of the water-soluble thiol ligand in deionized water (3 mL).[65] For ligand exchange reactions using *ω-carboxyalkylthiols*, the aqueous layer was buffered to pH 8 using a 0.1 mM KH_2PO_4/K_2HPO_4 buffer. The biphasic reaction mixture was stirred rapidly at room temperature until completion of the ligand exchange reaction (which can be monitored by the transfer of the darkly colored nanoparticles from the organic to the aqueous phase). The reaction time depends on the incoming ligand and typically varies from 1 h (for short-chain, charged thiols) up to 8 h (for long-chain, neutral thiols). Upon completion of the exchange reaction the layers were separated, and the aqueous layer was washed with dichloromethane (3 × 5 mL). The aqueous phase was evaporated under a stream of nitrogen at room temperature. The crude material was dissolved in the minimum amount of water and purified by gel filtration chromatography (Sephadex LH-20) to remove residual gold salts and excess free ligand. Alternatively, the crude product can be purified by ultracentrifugation at 340000*g*. The purity of the product (as indicated by the absence of free ligand and molecular gold species) is determined by ^{1}H NMR spectroscopy, and the material can be further characterized by UV−vis spectroscopy, XPS, TGA, and TEM (vide infra).

(1) 1-Azido-2,4-dinitrobenzene. This compound was synthesized according to literature.[61] ^{1}H NMR ($CDCl_3$): δ 7.51 (d, 1H, ^3J = 8.9 Hz), 8.47 (dd, 1H, ^3J = 8.9 Hz, ^4J = 2.7 Hz), 8.81 (d, 1H, ^4J = 2.6 Hz). UV−vis ($CHCl_3$): λ_{max} 262, 304 nm.

(2) 2,4-Dinitrophenylimino(triphenyl)phosphorane. This compound is the product of trapping PPh_3 with 1-azido-2,4-dinitrobenzene. An authentic sample for characterization purposes was prepared by mixing PPh_3 (12.3 mg, 0.05 mmol) with 1-azido-2,4-dinitrobenzene (9.7 mg, 0.05 mmol) in $CHCl_3$ (10 mL). After 30 min at room temperature, the solvent was evaporated, and the residue was washed with 20 mL of cold $CHCl_3$. The physical characterization agrees with the literature.[66] Combination of ^{1}H and ^{1}H{^{31}P} NMR ($CDCl_3$): δ 6.37 (dd, 1H, $^3J_{H-H}$ = 9.3 Hz, $^4J_{H-P}$ = 1.2 Hz), 7.53 (dt, 6H, ^3J = 7.5 Hz, $^4J_{H-P}$ = 3.3 Hz), 7.63 (ddt, 3H, $^3J_{H-H}$ = 7.2 Hz, $^4J_{H-H}$ = 2.4 Hz, $^5J_{H-P}$ = 2.4 Hz), 7.76 (ddd, 6H, $^3J_{H-P}$ = 12.6 Hz, $^3J_{H-H}$ = 7.2 Hz, $^4J_{H-H}$ = 2.4 Hz), 7.81 (dd, 1H, $^3J_{H-H}$ = 9.0 Hz, $^4J_{H-H}$ = 3.0 Hz), 8.63 (dd, 1H, $^4J_{H-H}$ = 2.7 Hz, $^5J_{H-P}$ = 3.0 Hz). ^{31}P{^{1}H} NMR ($CDCl_3$): δ 9.28. UV−vis ($CHCl_3$): λ_{max} 261, 376 nm.

(3) Chlorotriphenylphosphine Gold(I), $AuCl(PPh)_3$. The Au(I) complex was synthesized according to a known procedure.[67] The physical characterization is in agreement with the literature.[68] UV−visible extinction data (CH_2Cl_2; ϵ (mol^{-1} dm^3 cm^{-1})): 2.04×10^4 (235 nm); 2.57×10^3 (268 nm); 1.93×10^3 (275 nm). ^{13}C NMR ($CDCl_3$): δ 128.84 (d, $^1J_{C-P}$ = 62.4 Hz), 129.43 (d, $^{2/3}J_{C-P}$ = 12.1 Hz), 134.33 (d, $^{2/3}J_{C-P}$ = 14.1 Hz), 132.19 (d, $^4J_{C-P}$ = 2.0 Hz). ^{31}P{^{1}H} NMR ($CDCl_3$): δ 32.97 (s). R_f (CH_2Cl_2, silica): 0.82.

(4) Chlorobis(triphenylphosphine)gold, $[Au(PPh_3)_2]^+Cl^-$. This compound was synthesized according to a known procedure.[68] The physical data agree with those reported elsewhere.[68] ^{1}H NMR ($CDCl_3$): δ 7.46 (dt, 6H, $^3J_{HH}$ = 7.5 Hz, $^4J_{HP}$ = 3 Hz), 7.55 (dtt, 3H, $^3J_{HH}$ = 7.5 Hz, $^5J_{HP}$ = 2.7 Hz, $^4J_{HH}$ = 2.7 Hz), 7.67 (ddd, 6H, $^3J_{HP}$ = 12.3 Hz, $^3J_{HH}$ = 7.2 Hz, $^4J_{HH}$ = 2.1 Hz). ^{31}P{^{1}H} NMR ($CDCl_3$): δ 29.71 (s).

NMR Monitoring of Ligand Exchange between 1.5-nm Au_n−TPP and ODT. (A) General Procedure of Monitoring the Ligand Exchange between 1.5-nm Au_n−TPP and ODT by NMR. Distilled ODT was placed in an NMR tube and dissolved in $CDCl_3$. A ^{1}H NMR spectrum was obtained as a starting point for the reaction. The contents of the NMR tube were then added to a scintillation vial charged with 1.5-nm Au_n−TPP. The resulting mixture was quickly agitated until everything had dissolved and placed back into the NMR tube. The NMR tube was returned to the instrument and reshimmed, and spectra were collected at preset time intervals (the first spectrum was typically collected approximately 1 min after mixing).

(B) Monitoring of Ligand Exchange between 1.5-nm Au_n−TPP and Excess ODT. A solution of ODT (3.0 mg, 10 μmol) in $CDCl_3$ (0.6 mL) was added to 1.5-nm Au_n−TPP (5 mg, 20 nmol) and the reaction monitored by ^{1}H NMR spectroscopy. The first spectrum was recorded at t_0 = 1 min, followed by a spectrum every 1 min for a total time of 625 min.

(C) Monitoring of Ligand Exchange between 1.5-nm Au_n−TPP and Stoichiometric Amount of ODT to Replace All Nanoparticle-Bound Phosphines. A solution of ODT (3.0 mg, 10 μmol) in $CDCl_3$ (0.6 mL) was added to 1.5-nm Au_n−TPP (10 mg, 40 nmol) and the reaction monitored by ^{1}H NMR spectroscopy. The first spectrum was recorded at t_0 = 1 min followed by a spectrum every 1 min for a total time of 625 min.

(D) Monitoring of Ligand Exchange between 1.5-nm Au_n−TPP and ODT in the Presence of Excess PPh_3. A solution of ODT (3.0 mg, 10 μmol) and PPh_3 (10 mg, 40 μmol) in $CDCl_3$ (0.6 mL) was added to 1.5-nm Au_n−TPP (10 mg, 40 nmol) and the reaction monitored by ^{1}H NMR spectroscopy. The first spectrum was recorded at t_0 = 1 min followed by a spectrum every 1 min for a total time of 625 min.

(E) Trapping Experiment for Free PPh_3 Using 1-Azido-2,4-dinitrobenzene. A solution ODT (10.0 mg, 35 μmol) and 1-azido-2,4-dinitrobenzene (2 mg, 1 μmol) in $CDCl_3$ (0.6 mL) was added to 1.5-nm Au_n−TPP (10 mg, 40 nmol) and the reaction monitored by ^{1}H NMR spectroscopy. The first spectrum was recorded at t_0 = 1 min followed by a spectrum every 1 min for a total time of 625 min.

Acknowledgment. Support for this work was provided by the National Science Foundation (Grant DMR-9705343). We gratefully acknowledge C. Creutz for stimulating and helpful discussions.

(64) Schmid, G. *Inorg. Synth.* **1990**, *27*, 214−218.
(65) For thiols with low molecular weight such as propanethiol or mercaptoacetic acid, it is recommended to use only 10−15 mg of thiol to 20 mg of nanoparticle in order to avoid partial nanoparticle decomposition due to too much excess of thiol.
(66) Onys'ko, P. P.; Proklina, N. V.; Prokopenko, V. P.; Gololobov, Y. G. *Zh. Obshch. Khim.* **1984**, *54*, 325−333.
(67) Braunstein, P.; Lehner, H.; Matt, D. *Inorg. Synth.* **1990**, *27*, 218−221.
(68) Hussain, M. S.; Hossain, M. L.; Al-Arfaj, A. *Transition Met. Chem.* **1990**, *15*, 120−125.

Supporting Information Available: UV−visible spectra, TEM images, NMR spectra, and TGA data of representative nanoparticle samples, UV−visible spectra of $AuCl(PPh_3)$ and 1.5-nm Au_n−TPP, analysis of the ligand/gold ratio as a function of the thiol ligand, and discussion of the literature precedence for line broadening of ^{31}P NMR signals of PPh_3 caused by intermolecular phosphine exchanges (PDF). This material is available free of charge via the Internet at http://pubs.acs.org.

JA0457718